12-1-2011

Bi-Stability, Hysteresis, and Memory of Voltage-Gated Lysenin Channels

Daniel Fologea
Boise State University

Eric Krueger
University of Arkansas

Yuriy I. Mazur
University of Arkansas

Christine Stith
University of Arkansas

Yui Okuyama
University of Arkansas

See next page for additional authors

Authors
Daniel Fologea, Eric Krueger, Yuriy I. Mazur, Christine Stith, Yui Okuyama, Ralph Henry, and Greg J. Salamo

Bi-Stability, Hysteresis, and Memory of Voltage-Gated Lysenin Channels

Daniel Fologea
Boise State University

Eric Krueger, Yuriy I. Mazur, Christine Stith, Yui Okuyama, Ralph Henry, and Greg J. Salamo
University of Arkansas

Abbreviations. BLM, Bilayer Lipid Membrane; I-V, current-voltage; P_{open}, open probability; PFP, pore-forming protein; PFT, pore-forming toxin; $V_{1/2}$, midway voltage of activation.

Abstract

Lysenin, a 297 amino acid pore-forming protein extracted from the coelomic fluid of the earthworm *E. foetida*, inserts constitutively open large conductance channels in natural and artificial lipid membranes containing sphingomyelin. The inserted channels show voltage regulation and slowly close at positive applied voltages. We report on the consequences of slow voltage-induced gating of lysenin channels inserted into a planar Bilayer Lipid Membrane (BLM), and demonstrate that these pore-forming proteins constitute memory elements that manifest gating bi-stability in response to variable external voltages. The hysteresis in macroscopic currents dynamically changes when the time scale of the voltage variation is smaller or comparable to the characteristic conformational equilibration time, and unexpectedly persists for extremely slow-changing external voltage stimuli. The assay performed on a single lysenin channel reveals that hysteresis is a fundamental feature of the individual channel unit and an intrinsic component of the gating mechanism. The investigation conducted at different temperatures reveals a thermally stable reopening process, suggesting that major changes in the energy landscape and kinetics diagram accompany the conformational transitions of the channels. Our work offers new insights on the dynamics of pore-forming proteins and provides an understanding of how channel proteins may form an immediate record of the molecular history which then determines their future response to various stimuli. Such new functionalities may uncover a link between molecular events and macroscopic processing and transmission of information in cells, and may lead to applications such as high density biologically-compatible memories and learning networks.

Keywords: lysenin, voltage-gated channels, hysteresis, memory, pore-forming toxins

1. Introduction

Proteins and peptides that form membrane spanning pores and channels are essential for life [1, 2]. Although their primary role is to selectively traffic ions and molecules across the cell membrane, their activity is crucial in sustaining fundamental processes such as maintaining the electrochemical gradients across the cell membrane, generating the electrical impulses in nerves and other excitable cells, or actively participating in energy production processes [2]. Each particular functional feature of a PFP is related to a specific biological functionality, and their exploration may prove fruitful in deciphering novel yet inscrutable biological implications of such biomolecular structures. One of the most intriguing and less understood features expressed by PFPs specializing in ionic transport (ion channels) is their bi-stability manifested as hysteresis in conductance observed in response to variable external voltages [3-5]. The importance of such manifestation resides in the fact that hysteresis is the main mechanism exploited in data storage and emerging memory applications [6-8]. The exploration of such functionalities at biomolecular levels may uncover a link between molecular events and macroscopic processing and transmission of information in cells in the absence of a brain [9]. The dynamic break in symmetry and the resulting hysteresis in artificial systems are due to the competing time scales between the period of an oscillating external perturbation and the typical relaxation time of the system [10]. Voltage-gated ion channels are no exception and show dynamic hysteretic conductance when direct competition between the period of the oscillating applied voltage and the characteristic relaxation time of the conformational transitions from open to close states occurs [3-5, 11, 12]. This

phenomenon may have profound implications in deciphering new biological functions attributable to PFPs and ion channels, but insightful explorations in this field are rather scarce. The lack of availability of purified channels, their often difficult insertion and low stability in an artificial environment, along with fast conformational equilibration in response to external voltages impeded a real advancement in understanding such new features. Moreover, patch-clamp experiments performed on ultra-slow voltage-inactivated ion channels reveal the hysteretic behavior [3, 13, 14] but the missing analysis with regard to time or temperature dependence makes understanding its origin difficult. In this line of inquiries, we searched for other voltage-responsive PFPs that possess similar features to ion channels and allow extended analysis in artificial planar BLMs.

We focused the attention on lysenin, a 297 amino acid PFP extracted from the earthworm *E. foetida* [15, 16] that shares many important features of ion channels like voltage-regulation and high transport rate [17-19]. Lysenin self-inserts into cell membranes and artificial lipid bilayers containing sphingomyelin to form large uniform and stable channels (~3 nm diameter) [15-19] upon oligomerization of six monomer protein units. Owing to its high toxicity against vertebrates and hemolytic activity for red blood cells, lysenin is often referred as a PFT posing a defensive physiological role. Although considered ineffective against invertebrates [20-22], lysenin demonstrates a slight anti-bacterial activity, but the sphingomyelin-independent permeabilization does not lead to the formation of defined oligomeric structures [23].

Unfortunately, there is no high resolution structural data currently available for lysenin. Various experimental and theoretical approaches indicate that the protein contains ~55% β-structures [15, 24]. Common features such as the lack of hydrophobic stretches and the ability to organize highly-ordered and stable oligomeric pores suggest a direct comparison with the class of β-barrel channels [25-28]. However, lysenin does not share sequence similarities with other known PFTs, and the requirement of sphingomyelin as a specific membrane acceptor for oligomerization and pore formation is unique.

Symmetrical voltage-induced gating is considered a fundamental feature of porins and β -barrel pores [25]. However, asymmetrical voltage gating has been observed for bacterial porins, but their sustained inactivation occurs in response to high transmembrane voltages [25, 29, 30]. The lysenin channels' asymmetrical I-V characteristic shows a strong non-linearity in a narrow voltage range (rather similar to α-helical voltage-gated channels), and the discrete and uniform current blockages measured through individual channels are thought as conformational transitions that accompany the voltage induced toggle from the open to the closed state [18]. Lysenin channels exhibit very slow equilibration of a voltage-dependent step in the gating mechanism [18] and slow inactivation (channel closing) is observed as decreases in macroscopic currents at low positive holding potentials (>20 mV) [17, 18]. We hypothesized that such slow conformational equilibration of lysenin channels can induce hysteretic conductance in response to variable external voltages as predicted by the analytical model advanced by Pustovoit, *et al*. [12], thus providing the physical requirements for lysenin channels to potentially express bio-molecular memory. We investigated the lysenin channels' response to oscillatory voltage stimuli, and our exploration unveiled inscrutable functionalities and dynamic changes that may prove useful in deciphering new physiological implications of voltage-gated PFPs.

2. Materials and Methods

The BLM chamber consisted of two Teflon reservoirs (1 ml each) separated by a thin Teflon film in which we fabricated a ~70 μm diameter hole by using an electric spark. The BLM was composed of Asolectin, Sphingomyelin, and Cholesterol dissolved in n-decane in a 1:1:0.5 weight ratios [17, 18], and formed by using the painting method. If not otherwise indicated, 135 mM NaCl buffered with 20 mM Hepes, pH 7, was used as the support electrolyte. The electrical connections were completed by two Ag/AgCl electrodes inserted into the electrolyte solution on each side and connected to the headstage of an Axopatch 200B amplifier (Molecular Devices). Membrane currents were recorded under voltage clamp conditions and digitized using a DigiData 1440A digitizer and pClamp10 software (Molecular Devices). The channels were inserted into the BLM by adding lysenin (final concentration 0.2 nM, used as purchased from Sigma) to the grounded reservoir. Channel insertion was observed by recording the ionic open currents at -90 mV bias voltage (Fig. S1A). After a stable open current was obtained in less than 1 hour (Fig. S1B), the grounded reservoir was flushed with 20 ml fresh electrolyte to remove the non-inserted proteins. The slow equilibration of lysenin channels was assessed by measuring the macroscopic currents as a function of time in response to step voltages, and the hysteretic behavior was demonstrated by using linear and symmetrical triangle-shaped voltage ramps defined in the Episodic Stimulation Protocol, with the

sampling rate chosen to yield at least 2000 samples/run. The cut-off frequency of the low pass filter was set individually for each experiment to be at least ten times higher than the sampling frequency. Except for the variable-temperature experiment, the measurements were performed at room temperature (22±0.5 ^{0}C). When required, the temperature was controlled by a Planar Lipid Bilayer Thermocycler (Warner Instruments) and continuously monitored with a digital thermometer. Continuous stirring of the solutions in the BLM chamber was assured by a low noise magnetic stirrer (Spin-2 Stirplate, Warner Instruments). The acquired data were further analyzed using Clampfit 10.2 and Origin 8.

3. Results and Discussions

3.1 Slow equilibration of lysenin channels in response to external voltages

Slow equilibration of conformational changes that switch the ion channels from the conducting to the non-conducting state in response to external voltage stimuli is an essential condition for observing dynamic hysteresis in macroscopic currents [12]. External positive voltages close the lysenin channels and result in a slow but sustained decrease in the macroscopic currents [18]. However, the channels' reopening and reinstatement of conducting properties in response to appropriate voltages have been consistently neglected.

The macroscopic current (I) through a population of uniform lysenin channels in response to step voltages (neglecting the capacitive component) is dependent on the applied voltage (V), the unitary conductance of an individual channel (g_0), and the instantaneous number of open channels in the population [31]:

$$I = Vg_0 NP_{open}(V,t) \quad (1)$$

where N is the total number of pores in the population..

The evolution of the open probability after a discrete voltage change is described by [11]:

$$P_{open}(t) = P_{eq} - (P_{eq} - P_i)\exp(-t/\tau) \quad (2)$$

where P_i is the open probability at the previous voltage, and P_{eq} denotes the equilibrium open probability at the new voltage. The above relationships were used to estimate the time constant (τ) from the current traces recorded in response to various voltage steps.

When we applied a positive step voltage (+60 mV) across a BLM containing a population of inserted lysenin channels, the macroscopic current slowly decreased and indicated that the channels closed (Fig. 1) [17, 18]. The large value of the time constant ($\tau \sim 11$ s) corresponding to closing (inactivation) demonstrated that the lysenin channels' conformational changes were much slower compared to ion channels [5, 32]. The reopening of the voltage-closed channels (reactivation) was initiated by subsequent application of either negative or low positive voltages (Fig.1). Although the channels' reactivation was faster in response to an applied step voltage of -60 mV than an applied step voltage of +10 mV, neither of these processes were relatively rapid and required between 10 seconds and 1 minute to reach the equilibrium. This first experiment demonstrated that both inactivation and reactivation of lysenin channels in response to external voltages are slow processes, which constitutes the prerequisite for a dynamic hysteretic response in conductance [12].

3.2 The voltage sweep rate modulates the hysteresis in macroscopic currents

To further analyze the influence of the voltage rate on inactivation and reactivation and to observe the predicted hysteresis, we measured the macroscopic currents through a population of lysenin channels in response to linear-variable voltage ramps with voltage rates ranging from 1 Vs^{-1} to 0.025 mVs^{-1} and amplitudes up to 100 mV. Rapid voltage ramps (1 Vs^{-1}) yielded ohmic and identical I-V curves over the entire voltage range (Fig. 2A) for both ascending (inactivation curve) and descending voltage (reactivation curve) applications. The linearity and the constant slopes of the resultant curves indicated negligible changes in the conducting state of each channel during the voltage stimulation. We concluded that the time scale of the stimulus was much shorter than the characteristic equilibration time of lysenin channels, and the rapid voltage variation did not allow the channels to adjust their

conformation in response to instantaneous voltages and close. Consequently, the lack of inactivation during the rapid voltage stimulation resulted in a linear and symmetrical response.

A one hundred-fold decrease in the voltage rate to 0.01 Vs^{-1} affected the response linearity and broke the symmetry (Fig. 2B). The initial I-V curve in its pre-switching state (V < 40 mV) exhibited an ohmic characteristic and indicated that even when the bias voltage exceeded the effective threshold required to promote switching (~20 mV) [17, 18] the channels did not close because the application time was shorter than the required equilibration time. Nevertheless, the non-linear current response at voltages greater than ~40 mV indicated that the positive voltages in this range promoted channel inactivation, and this switching to the non-conducting state was reflected in the monotonically decreasing currents while increasing the applied voltage. Descending voltages yielded macroscopic currents that followed a different I-V trajectory. At the beginning of the descending ramp, the macroscopic current decreased faster than the descending voltage and indicated a continuation of channel closure. Eventually, further decrease in the applied voltage initialized channel reactivation observed as an increase in conductance while decreasing the voltage. However, the resulting currents were lower than those recorded during the ascending ramp until the applied voltage decreased to a few mV where the I-V characteristic regained its ohmic attribute and overlapped the inactivation curve.

The bi-stability seen as a distinctive split of the stimulus-response relationship between the macroscopic currents recorded during the linearly swept ascending and descending voltages demonstrated the predicted hysteresis in conductance. Apparently, the non-symmetrical response originated in the dynamic hysteresis introduced by the lag between the voltage variation and the dynamic conformational equilibrium, and open-close transitions occurred only in response to sufficiently slow voltage changes. A salient feature of dynamic hysteresis resulting solely from slow equilibration is that it should vanish in the limiting cases of very rapid and very slow voltage variations [11, 12]. We observed that the ascending and descending I-V curves collapsed to indiscernible straight lines when the voltage changed rapidly, while slower voltage variations induced a hysteretic behavior. A further reduction in the voltage rates to 0.2 mVs^{-1} and 0.05 mVs^{-1} (Fig. 2C, D) accentuated the non-linearity and produced steeper transitions from the conducting to the non-conducting regimes, observed as dynamic negative differential resistances [17]. Nevertheless, the non-symmetrical response remained, although the time-scale of the voltage stimulus was much larger than the characteristic relaxation time of the lysenin channels, and suggested a small persisting hysteresis. The hysteresis in conductance was fully reflected in the open probability extracted from the corresponding macroscopic current [31-33] recorded during inactivation and reactivation at 0.2 mVs^{-1} (Fig. 2E). The observed leftward shift of P_{open} for descending voltages and the ~11 mV displacement in $V_{1/2}$ were consistent with the macroscopic current hysteretic response.

Further analysis of the hysteresis dependency on the voltage rate in terms of loop area as a measure of hysteresis (Fig. 2F) confirmed two of the principal attributes of dynamic hysteresis [12]: its disappearance for fast voltage variations, and the characteristic bell shape. However, the macroscopic current response stabilized for voltage rates less than 0.2 mVs^{-1}, and the loop area asymptotically decreased to a small but non-zero value contrary to the dynamic hysteresis model predictions [12]. The hysteresis in conductance was expected to completely disappear when the period of the oscillatory voltage stimulus greatly exceeded the characteristic relaxation time of lysenin channels, which did not happen. To check the hysteresis persistency at exceedingly longer time scales we measured the macroscopic current in response to a very slow changing voltage (~3.3 μVs^{-1}) (Fig. 3). Although the period of the variable voltage stimulus (~48000 s) greatly exceeded (by several orders) the characteristic equilibration time of the lysenin channels, a small yet stable hysteresis was observed and indicated the possibility of one or more supplementary hidden steps in the gating mechanism as a source of the long delay. Alternatively, the persistent bi-stability could be explained by considering a static hysteresis in conductance as a fundamental intrinsic feature of the lysenin gating mechanism. To discriminate between the two possibilities, the experiments should be performed at time scales much larger than what used, but the well known instability of an unsupported BLM impeded that investigation.

3.3 The hysteresis in conductance is an intrinsic property of a single lysenin channel

Next, we investigated hysteresis as an intrinsic characteristic of an individual channel versus a population of channels by conducting the experiments on a single channel. The classical approach to estimate P_{open} from the dwell time at fixed transmembrane potentials [5, 34, 35] proved difficult owing to the very low transition frequency. This limitation was circumvented by determining the instantaneous probability of the single channel to be open or closed

at various voltages during voltage ramp stimulation. A corresponding probability (1 for open, 0 for closed) was assigned to each voltage value by observing the current and determining the conducting state, and the average probability was calculated from multiple runs. In order to reduce the dynamic component of the hysteresis, we used a low rate of voltage change (0.1 mVs^{-1}). The current recorded successively through the same single-channel for both ascending and descending voltage stimuli (see a typical run in Fig. 4A) showed that the channel behavior can be approximated as a two state system, and reactivation occurred at a lower voltage than inactivation. The average P_{open} of a single channel (Fig. 4B) showed a leftward shift during reactivation and a bi-stability similar to that observed for an entire population of lysenin channels (see Fig. 2E). Therefore, the hysteresis observed for a population of lysenin channels was a consequence of the hysteresis in the open probability of a single channel.

A population of lysenin channels act as two-terminal controlled switches that adopt multiple resistance states in response to applied voltages [17] and manifest memory capabilities, which is the classical definition of memristance (memory-resistance) [36, 37]. Memristance has been predicted to serve as the foundation for understanding a multitude of non-linear behaviors previously observed in the I-V characteristics of nano-scale electronic devices, such as bipolar switching, negative differential resistance, or hysteretic conductance [38]. At the single channel level, each individual unit can be described as a nano-scale bi-stable system that has the potential to achieve one of two possible states characterized by different resistances dependent on the applied voltage and the history of the system. Hence, a lysenin channel has the ability to "remember" its previous state indicating intrinsic memory expressed by a simple bio-molecular nano-structure. Such memristive elements simulate the mechanisms of biological memory [39] and they may constitute the explanatory basis of the intelligent abilities and memory displayed by unicellular organisms [9] or other cells without involving brain functions.

3.4 Temperature effects on macroscopic currents through lysenin channels

The lack of knowledge regarding structural changes that accompany the conformational transitions resulting in lysenin ON-OFF switching constitutes a serious impediment in advancing any mechanistic model of the channel functionality. The resistance of each channel depends on external variables such as voltage and electrolyte conditions, and its instantaneous conducting state. The open-closed transition is conventionally considered a thermally driven process [40, 41] characterized by temperature-dependent kinetic rates related to one or more energy barriers separating individual states. To advance our understanding in deciphering the nature of lysenin channels bi-stability we examined the gating behavior and the hysteretic properties by conducting the I-V measurements at different temperatures (Fig. 5).

The voltage required to inactivate the lysenin channels decreased at higher temperatures, which was observed as a gradual leftward shift of the inactivation curve (Fig. 5A). The temperature influence on inactivation was confirmed by determining P_{open} from the macroscopic currents (Fig. 5B), and indicated a gradual rightward shift of P_{open} and $V_{1/2}$ displacement up to ~16 mV upon cooling. Unexpectedly, no lateral shift of reactivation was recorded during descending voltage ramps (Fig. 5C) for the entire temperature range, and P_{open} and $V_{1/2}$ remained virtually unchanged for the same conditions (Fig. 5D). Lysenin channels exhibited gating thermosensitivity similar to other ion channels [42-45] only during ascending voltage sweeps, while returning voltages indicated temperature-adamant open probabilities. We interpreted the temperature dependence based on the general principle of ion channels temperature sensitivity previously formulated by Voets *et al*. [43, 44]. According to this principle, the energies associated with channel opening and closing transitions must be sufficiently different to manifest temperature sensitivity, and less pronounced temperature sensitivity indicates similar transitional energy barriers. The open probability of lysenin channels expressed thermal sensitivity during ascending voltage ramps, and this response suggested different energy barrier heights for opening and closing. On the contrary, the open probability during descending voltage ramps demonstrated negligible temperature influence and suggested similar energy barrier heights for channel closing and opening. These intriguing results can be explained by accounting for major dynamic differences in the free energy profiles corresponding to inactivation and reactivation, which may be consequences of conformational transitions, of the time elapsed in a particular state, or of the direction of the voltage changes [3].

These findings establish a link between the hysteretic behavior and the unusual temperature dependency. The reopening of lysenin channels during descending voltages is realized through an invariant I-V trajectory. The persisting hysteresis stems from the stable reactivation pathway, which endows lysenin with unique properties and memory capabilities among PFPs and ion channels. The bi-stability of lysenin channels manifested not only in response to external voltages but in response to temperature changes as well, and we did not identify any previous

reports of similar properties of other PFPs, including ion channels. The classical kinetic diagrams and energy levels described by Markov processes [40] cannot adequately describe these properties, and new dynamical approaches must be developed for a true understanding of such new and unexpected functionalities [46, 47].

4. Conclusions

Previous work on voltage-gated channels do not report hysteresis in conductance that persists at such large time scales, especially those exceeding the characteristic relaxation time of the conformational equilibration [3-5]. Moreover, lysenin is neither an ion channel nor a transmembrane protein in its native environment, and its physiological role is still uncertain. Its cytolytic activity suggests a PFT, but when inserted into artificial BLMs lysenin replicates fundamental properties of ion channels that do not match the classic profile of PFTs. It is difficult to understand why a lethal PFT would close and lose its lytic activity in response to certain transmembrane potentials [17, 18] or in the presence of very low concentrations of multivalent cations [48]. Such intricate functionalities complicate any attempt to elucidate its true physiological role and the novel features unveiled in this work only adds to its obscurity. The complex response to voltage, multivalent ions, and temperature suggests strong and multi-potent sensing capabilities but there is no data supporting such a physiological role.

Lysenin channels demonstrate memory capabilities by exhibiting multiple resistance states dependent on the applied voltage and their history. The assay conducted on artificial BLMs demonstrated that hysteresis and memory are inherent features of the lysenin channels gating mechanism rather than the result of an external biochemical regulatory factor. The concept of bio-molecular memory demonstrated in our study provides an understanding of how channel proteins found in living cells may form an immediate record of the molecular history which then determines their future response to various stimuli. We anticipate this study will initiate expanded investigations aimed at identifying similar functionalities of ion channels to understand how their response to various stimuli is influenced by their molecular history. Other PFPs with similar features, especially ion channels, present in cell membranes may constitute the explanatory basis for cellular memory phenomena recently unveiled [9]. Further research will be required to extrapolate these findings to physiologically relevant ion channels such as HCN channels [4] or slow C-type inactivated channels [49]. In the meanwhile, we expect that our results will advance understanding in the obscure physiological role of lysenin and expand our knowledge regarding the functionality of pore forming toxins, while opening innovative approaches in developing smart bio-compatible nano-scale devices.

Acknowledgements

The authors acknowledge financial support from Howard Hughes Medical Institute (Grant 52005890) and NSF (Grant DMR-0520550).

Appendix A. Supplementary data

Supplementary data to this article can be found online.

References

[1] Q. Ren, I.T. Paulsen, Comparative Analyses of Fundamental Differences in Membrane Transport Capabilities in Prokaryotes and Eukaryotes, PLoS Comput. Biol. 1 (2005) 0190-0201.
[2] M.H.J. Saier, Families of transporters and their classification, in: M.W. Quick (Ed.), Transmembrane Transporters, Wiley-Liss, Inc., New Jersey, 2002, pp. 1-17.
[3] L. Kaestner, P. Christophersen, I. Bernhardt, P. Bennekou, The non-selective voltage-activated cation channel in the human red blood cell membrane: reconciliation between two conflicting reports and further characterization, Bioelectrochemistry 52 (2000) 117-125.
[4] R. Mannikko, S. Pandey, H.P. Larsson, F. Elinder, Hysteresis in the Voltage Dependence of HCN Channels: Conversion between Two Modes Affects Pacemaker Properties, J. Gen. Physiol. 125 (2005) 305-326.
[5] L.M. Nowak, J.M. Wright, Slow Voltage-Dependent Changes in Channel Open-State Probability Underlie Hysteresis of NMDA Response in Mg^{2+}-free solutions, Neuron 8 (1992) 181-187.
[6] W. Lu, C.M. Lieber, Nanoelectronics from the bottom up, Nat. Mater. 6 (2007) 841-850.
[7] R. Waser, M. Aono, Nanoionics-based resistive switching memories, Nat. Mater. 6 (2007) 833-840.
[8] U. Wurstbauer, C. Sliwa, D. Weiss, T. Dietl, W. Wegscheider, Hysteretic magnetoresistance and thermal bistability in a magnetic two-dimensional hole system, Nat. Phys. 6 (2010) 955-959.
[9] T. Saigusa, A. Tero, T. Nakagahi, Y. Kuramoto, Amoebae Anticipate Periodic Events, Phys. Rev. Lett. 100 (2008) 018101.
[10] H. Zhu, S. Dong, J.-M. Liu, Hysteresis loop area of the Ising model, Phys. Rev. B 70 (2004) 132403(132404).
[11] T. Andersson, Exploring voltage-dependent ion channels *in silico* by hysteretic conductance, Math. Biosci. 226 (2010) 16-27.
[12] M.A. Pustovoit, A.M. Berezhkovskii, S.M. Bezrukov, Analytical theory of hysteresis in ion channels: Two state model, J. Chem. Phys. 125 (2006) 194907.
[13] P. Bennekou, T.L. Barksmann, L.R. Jensen, B.I. Kristensen, P. Christopersen, Voltage activation and hysteresis of the non-selective voltage-dependent channel in the intact human red cell, Bioelectrochemistry 62 (2004) 181-185.
[14] P.S. Pennefather, W. Zhou, T.E. DeCoursey, Idiosyncratic Gating of HERG-like K^+ Channels in Microglia, J. Gen. Physiol. 111 (1998) 795-805.
[15] A.-B.A. Shakor, E.A. Czurylo, A. Sobota, Lysenin, a unique sphingomyelin-binding protein, FEBS Lett. 542 (2003) 1-6.
[16] A. Yamaji-Hasegawa, A. Makino, T. Baba, Y. Senoh, H. Kimura-Suda, S.B. Sato, N. Terada, S. Ohno, E. Kiyokawa, M. Umeda, T. Kobayashi, Oligomerization and pore formation of a sphingomyelin-specific toxin, lysenin, J. Biol. Chem. 278 (2003) 22762-22770.
[17] D. Fologea, E. Krueger, R. Lee, M. Naglak, Y. Mazur, R. Henry, G. Salamo, Controlled Gating of Lysenin Pores, Biophys. Chem. 146 (2010) 25-29.
[18] T. Ide, T. Aoki, Y. Takeuchi, T. Yanagida, Lysenin forms a voltage-dependent channel in artificial lipid bilayer membranes, Biochem. Biophys. Res. Commun. 346 (2006) 288-292.
[19] K. Kwiatkowska, R. Hordejuk, P. Szymczyk, M. Kulma, A.-B. Abdel-Shakor, A. Plucienniczak, K. Dolowy, A. Szewczyk, A. Sobota, Lysenin-His, a sphingomyelin-recognizing toxin, requires tryptophan 20 for cation-selective channel assembly but not for membrane binding, Mol. Membr. Biol. 24 (2007) 121-134.
[20] H. Kobayashi, N. Ohta, U. Masato, Biology of Lysenin, a Protein in the Coelomic Fluid of the Earthworm *Eisenia foetida*, International Review of Cytology 236 (2004) 45-99.
[21] H. Kobayashi, M. Ohtomi, Y. Sekizawa, N. Ohta, Toxicity of coelomic fluid of the earthworm *Eisenia foetida* to vertebrates but not invertebrates: probable role of sphingomyelin, Comparative Biochemistry and Physiology Part C 128 (2001) 402-411.
[22] N. Ohta, S. Shioda, Y. Sekizawa, Y. Nakai, H. Kobayashi, Sites of expression of mRNA for lysenin, a protein isolated from the coelomic fluid of the earthworm *Eisenia foetida*, Cell Tissue Research 302 (2000) 263-270.
[23] H. Bruhn, J. Winkelmann, C. Andersen, J. Andra, M. Leippe, Dissection of the mechanisms of cytolytic and antibacterial activity of lysenin, a defence protein of the annelid *Eisenia fetida*, Developmental and Comparative Immunology 30 (2006) 597-606.
[24] M. Herec, M. Gagos, M. Kulma, K. Kwiatkowska, A. Sobota, W.I. Gruszecki, Secondary structure and orientation of the pore-forming toxin lysenin in a sphingomyelin-containing membrane, Biochim. Biophys. Acta 1778 (2008) 872-879.
[25] G. Bainbridge, I. Gokce, J.H. Lakey, Voltage gating is a fundamental feature of porin and toxin β-barrel membrane channels, FEBS Lett. 431 (1998) 305-308.

[26] A. Basle, R. Iyer, A.H. Delcour, Subconductance states in OmpF gating, Biochim. Biophys. Acta 1664 (2004) 100-107.
[27] B.R. Cheneke, B. van den Berg, L. Movileanu, Analysis of Gating Transitions among the Three Major Open States of the OpdK Channel, Biochemistry 50 (2011) 4987-4997.
[28] M.M. Mohammad, L. Movileanu, Impact of Distant Charge Reversals within a Robust β -Barrel Protein Pore, J. Phys. Chem. B 114 (2010) 8750-8759.
[29] J.H. Lakey, F. Pattus, The voltage-dependent activity of *Escherichia coli* porins in different planar bilayer reconstitutions, Eur. J. Biochem. 186 (1989) 303-308.
[30] H. Samartzidou, A.H. Delcour, *E. coli* PhoE porin has an opposite voltage-dependence to the homologous OmpF, EMBO J. 17 (1998) 93-100.
[31] F. Bezanilla, The Voltage Sensor in Voltage-Dependent Ion Channels, Physiol. Rev. 80 (2000) 555-592.
[32] F. Bezanilla, Voltage-Gated Ion Channels, IEEE Trans. Nanobiosci. 4 (2005) 34-48.
[33] B. Nilius, K. Talavera, G. Owsianik, J. Prenen, G. Droogmans, T. Voets, Gating of TRP channels: a voltage connection?, J. Physiol. 567 (2005) 35-44.
[34] G. Ehrenstein, H. Lecar, R. Nossal, The nature of the Negative Resistance in Bimolecular Lipid Membranes Containing Excitability-Induced Material, J. Gen. Physiol. 55 (1970) 119-133.
[35] N. Mukhtasimova, W.Y. Lee, H.-L. Wang, S.M. Sine, Detection and trapping of intermediate states priming nicotinic receptor channel opening, Nature 459 (2009) 451-455.
[36] J. Borghetti, G.S. Snider, P.J. Kuekes, J.J. Yang, D.R. Stewart, R.S. Williams, 'Memristive' switches enable 'stateful' logic operations via material implication, Nature 464 (2010) 873-876.
[37] L.O. Chua, S.M. Kang, Memristive Devices and Systems, Proc. IEEE 64 (1976) 209-223.
[38] D.B. Strukov, G.S. Snider, D.R. Stewart, R.S. Williams, The missing memristor found, Nature 453 (2008) 80-83.
[39] Y.V. Pershin, S. La Fontaine, M. Di Ventra, Memristive model of amoeba learning, Phys. Rev. E 80 (2009) 021926.
[40] A. Correa, F. Bezanilla, R. Latorre, Gating Kinetics of Batrachotoxin-modified Na^+ channels in the squid giant axon, Biophys. J. 61 (1992) 1332-1352.
[41] F.J. Sigworth, Voltage gating of ion channels, Q. Rev. Biophys. 27 (1994) 1-40.
[42] R. Latorre, S. Brauchi, G. Orta, C. Zaelzer, G. Vargas, ThermoTRP channels as modular proteins with allosteric gating, Cell Calcium 42 (2007) 427-438.
[43] T. Voets, G. Droogmans, A. Janssens, V. Flockerzi, B. Nilius, The principle of temperature-dependent gating in cold- and heat-sensitive TRP channels, Nature 430 (2004) 748-754.
[44] T. Voets, K. Talavera, G. Owsianik, B. Nilius, Sensing with TRP channels, Nat. Chem. Biol. 1 (2005) 85-92.
[45] H. Xu, I.S. Ramsey, S.A. Kotecha, M.M. Moran, J.A. Chong, D. Lawson, P. Ge, J. Lilly, I. Silos-Santiago, Y. Xie, P.S. DiStefano, R. Curtis, D.E. Clapham, TRPV3 is a calcium-permeable temperature-sensitive cation channel, Nature 418 (2002) 181-186.
[46] L.S. Liebovitch, D. Scheurle, M. Rusek, M. Zochowski, Fractal methods to Analyze Ion Channel Kinetics, Methods 24 (2001) 359-375.
[47] D. Soudry, R. Meir, History-dependent dynamics in a generic model of ion channels - an analytic study, Frontiers in Computational Neuroscience 4, Article 3 (2010).
[48] D. Fologea, E. Krueger, R. Al Faori, R. Lee, Y.I. Mazur, R. Henry, M. Arnold, G.J. Salamo, Multivalent ions control the transport through lysenin channels, Biophys. Chem. 152 (2010) 40-45.
[49] L.G. Cuello, V. Jogini, D.M. Cortes, E. Perozo, Structural mechanism of C-type inactivation in K^+ channels, Nature 466 (2010) 203-208.

Figure legends

Fig. 1. Slow response of lysenin channels to step voltages is an essential condition for dynamic hysteresis in response to variable external voltages. (A) A positive step voltage of +60 mV slowly closes (inactivates) the channels. The closed channels reopen (reactivate) when a negative potential of -60 mV is applied across the bilayer. (B) The lysenin channels previously closed by a +60 mV step voltage slowly reopen (reactivate) in response to a low positive voltage step of +10 mV. The time constants (τ) were determined by fitting the experimental data with single-term exponential functions.

Fig. 2 The hysteresis in macroscopic currents through lysenin channels in response to external linear-variable voltage stimuli with various sweep rates (black: ascending voltage/inactivation curve, gray: descending voltage/reactivation curve). (A) 1 Vs^{-1}. (B) 0.01 Vs^{-1}. (C) 0.2 mVs^{-1}. (D) 0.05 mVs^{-1}. (E) The channels' open probability determined from (c) reflects the hysteresis in macroscopic current. (F) The variation of the hysteresis loop area (1 nW = 1 nA*1 V) as a function of voltage sweep rate (n = 2-10, ± s.d.).

Fig. 3. Long-term hysteresis in the voltage-induced gating of lysenin channels. The macroscopic current through lysenin channels determined during slow ascending (black) and descending (grey) voltage sweeps (~3.3 μVs^{-1}).

Fig. 4. The hysteresis in macroscopic currents is a consequence of the hysteretic response in the voltage-induced gating of a single lysenin channel (black: ascending voltage/inactivation curve, gray: descending voltage/reactivation curve, voltage sweep rate 0.1 mVs^{-1}). (A) A typical I-V curve recorded for a single lysenin channel that shows the gating hysteresis. (B) The single-channel open probability measured from the I-V curves recorded for a single channel (n = 140, ± s.e.m.).

Fig. 5. Macroscopic currents and open probabilities of lysenin channels in response to linear voltage ramps (0.1 mVs^{-1}) at different temperatures (as indicated in (A)). (A) Macroscopic currents recorded during ascending voltage ramps show a leftward shift in the inactivation curve when temperature increases. (B) The open probabilities calculated for ascending voltage ramps. (C) The macroscopic currents recorded during descending voltage ramps. (D) The open probabilities calculated for descending voltage ramps.

Supplementary Material

Lysenin inserts stable and uniform pores in BLMs

Addition of lysenin (final concentration 0.2 nM) to the grounded side of the BLM biased by -90 mV produced discrete changes in the open current (Fig. S1A), and the stepwise variations were interpreted as the insertion of individual lysenin channels into the BLM. Each insertion step was characterized by similar changes in the ionic current (32 ± 2.7 pA) indicating the channels' uniformity. The unitary conductance suggests that all the channels were structurally identical although no further purification of the commercial lysenin product was performed. The insertion process continued for about 40 minutes and then the open current stabilized (Fig. S1B). The removal of the un-inserted proteins by flushing the ground chamber with excess amounts of fresh buffered electrolyte did not change the open current and indicated the long-term stability of the inserted channels.

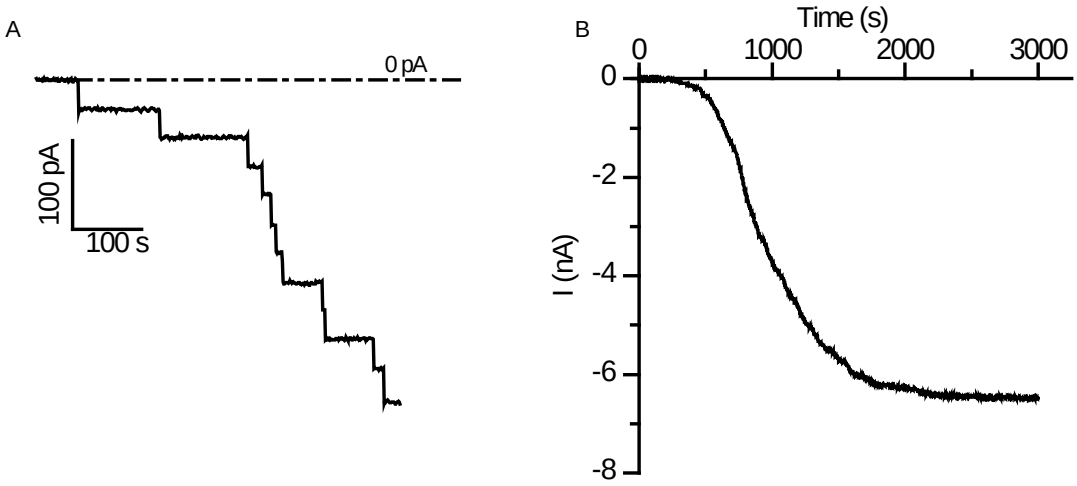

Fig. S1. Lysenin inserts stable and uniform pores in BLMs. A) The stepwise variation of the open current observed after lysenin addition to the ground side of the bilayer supports a mechanism of permeabilization based on uniform channel formation. B) The completion of the channel insertion process was achieved in less than 1 hour and indicated by the steady open current.

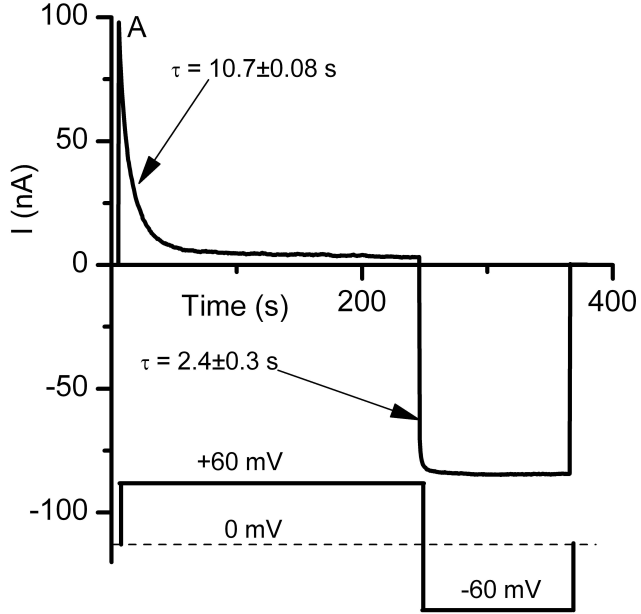
A
τ = 10.7±0.08 s
100
50
0
-50
-100
I (nA)
Time (s)
200
400
τ = 2.4±0.3 s
+60 mV
0 mV
-60 mV

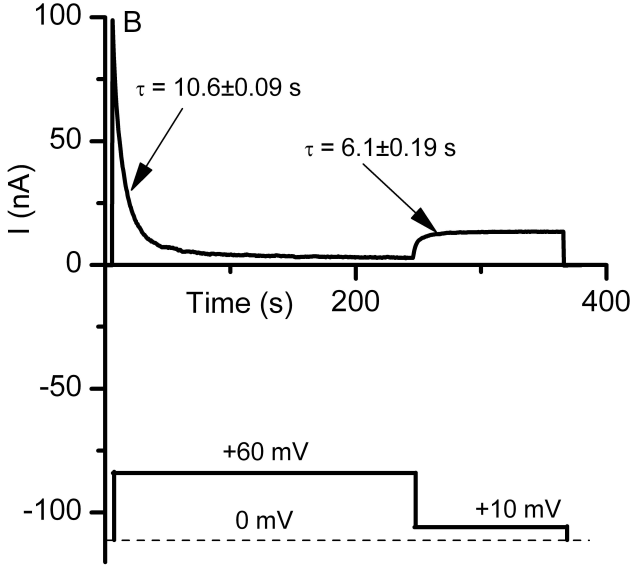
B
τ = 10.6±0.09 s
τ = 6.1±0.19 s
100
50
0
-50
-100
I (nA)
Time (s)
200
400
+60 mV
0 mV
+10 mV

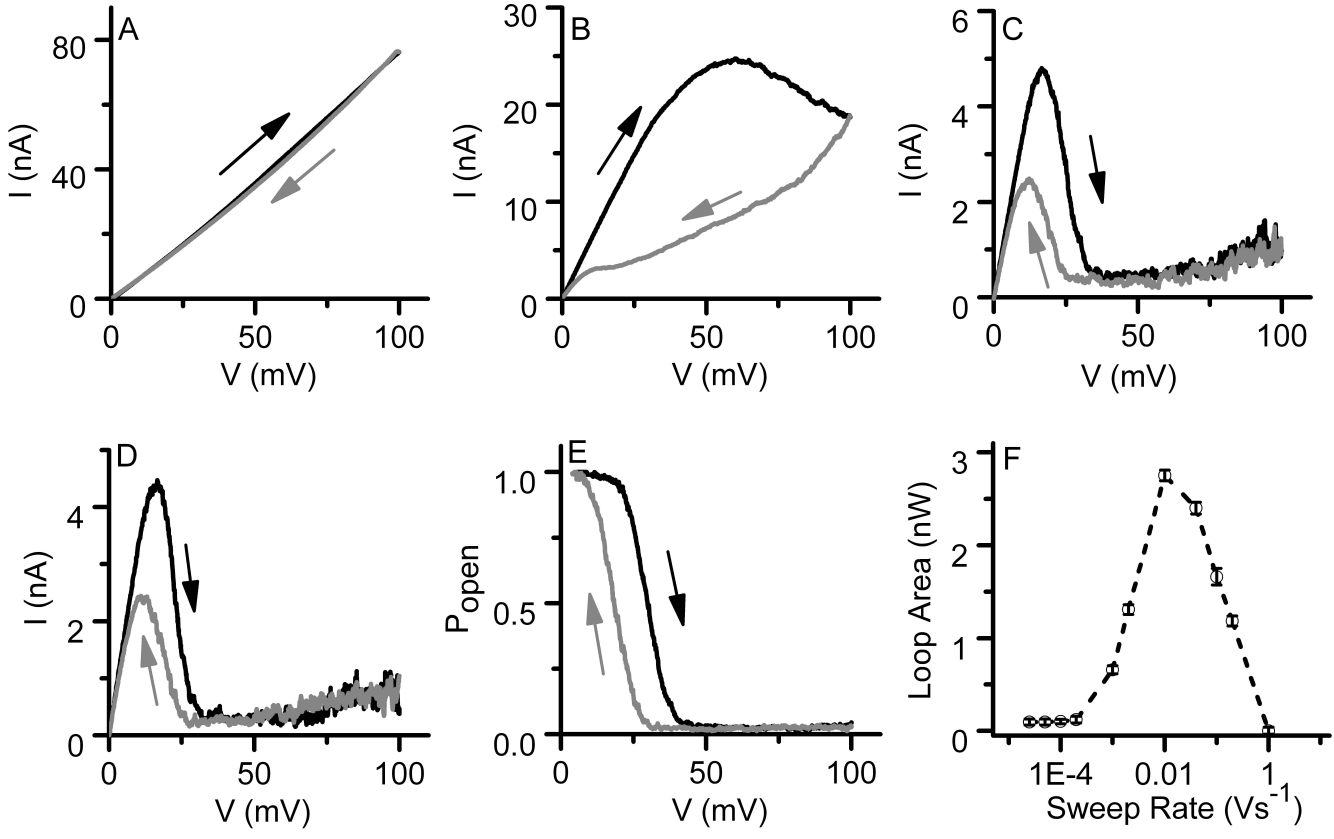
A
I (nA)
80
40
0
0
50
100
V (mV)
B
I (nA)
30
20
10
0
0
50
100
V (mV)
C
I (nA)
6
4
2
0
0
50
100
V (mV)
D
I (nA)
4
2
0
0
50
100
V (mV)
E
P open
1.0
0.5
0.0
0
50
100
V (mV)
F
Loop Area (nW)
3
2
1
0
1E-4
0.01
1
Sweep Rate (Vs-1)

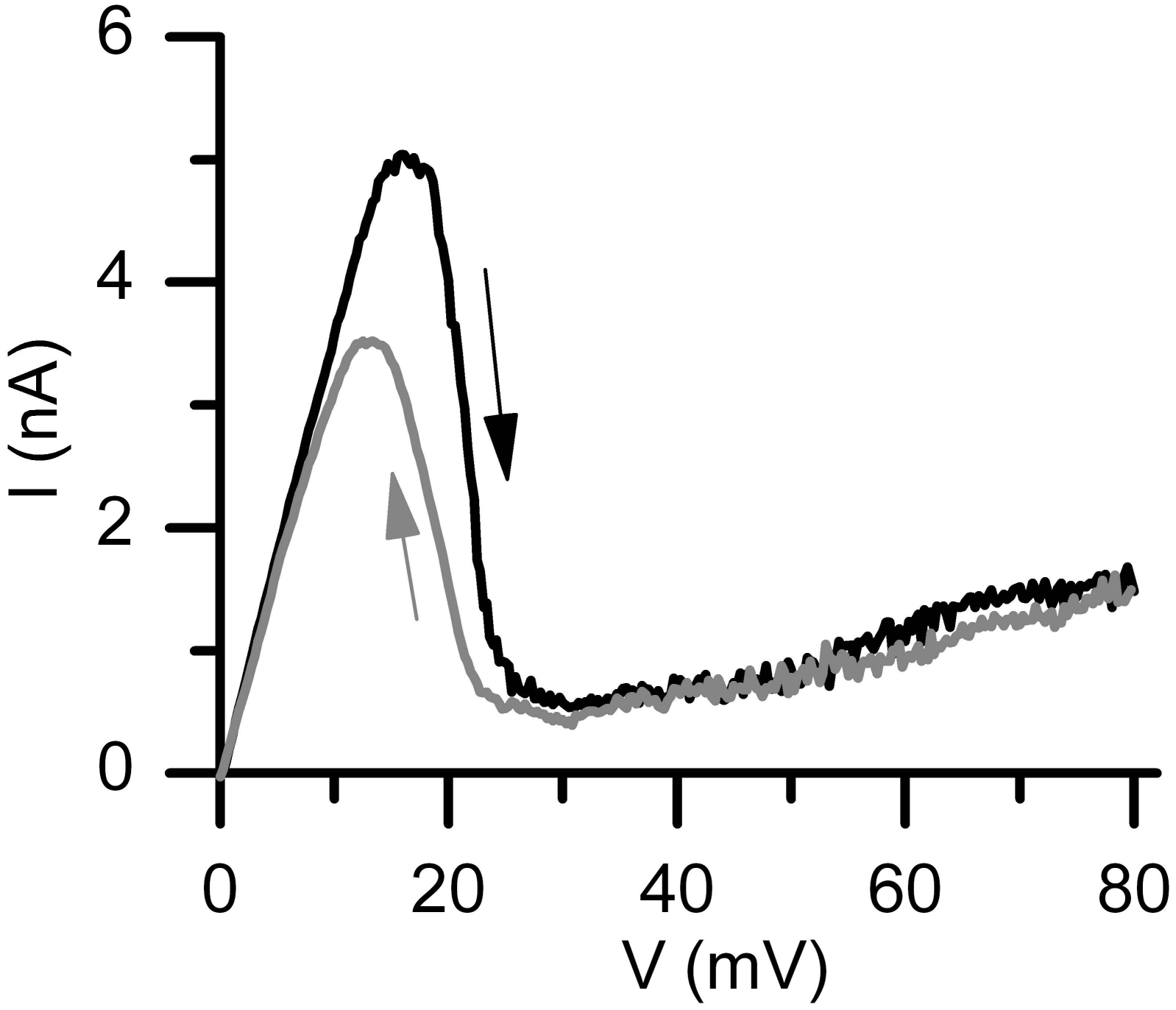
6
4
2
0
I (nA)
0
20
40
60
80
V (mV)

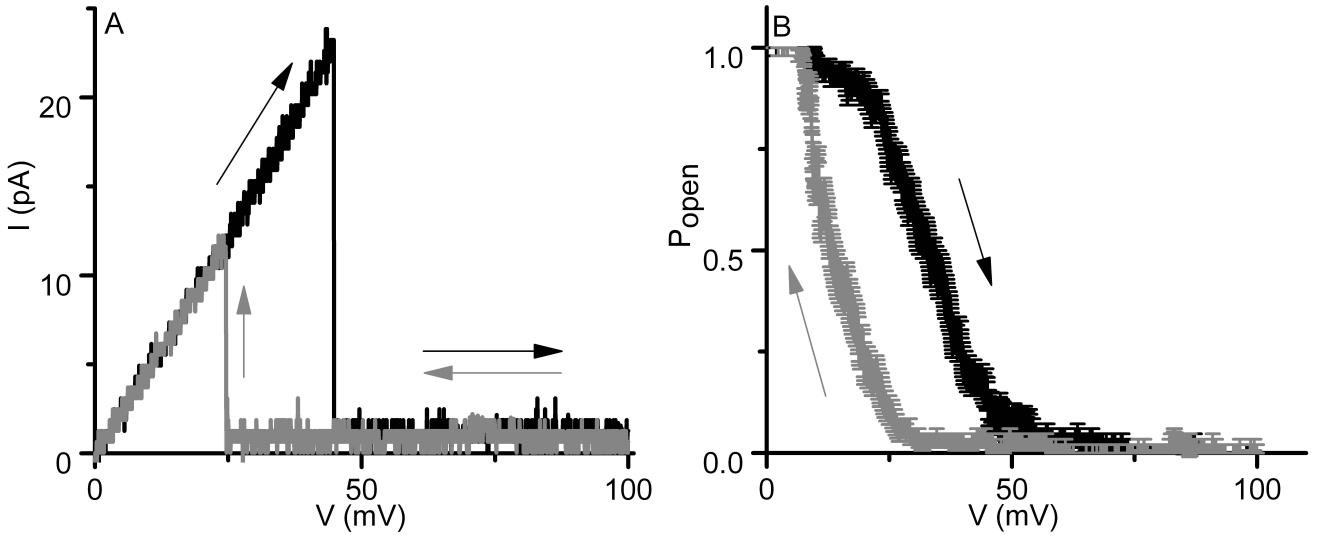
A
I (pA)
20
10
0
0
50
100
V (mV)
B
1.0
0.5
0.0
P open
0
50
100
V (mV)

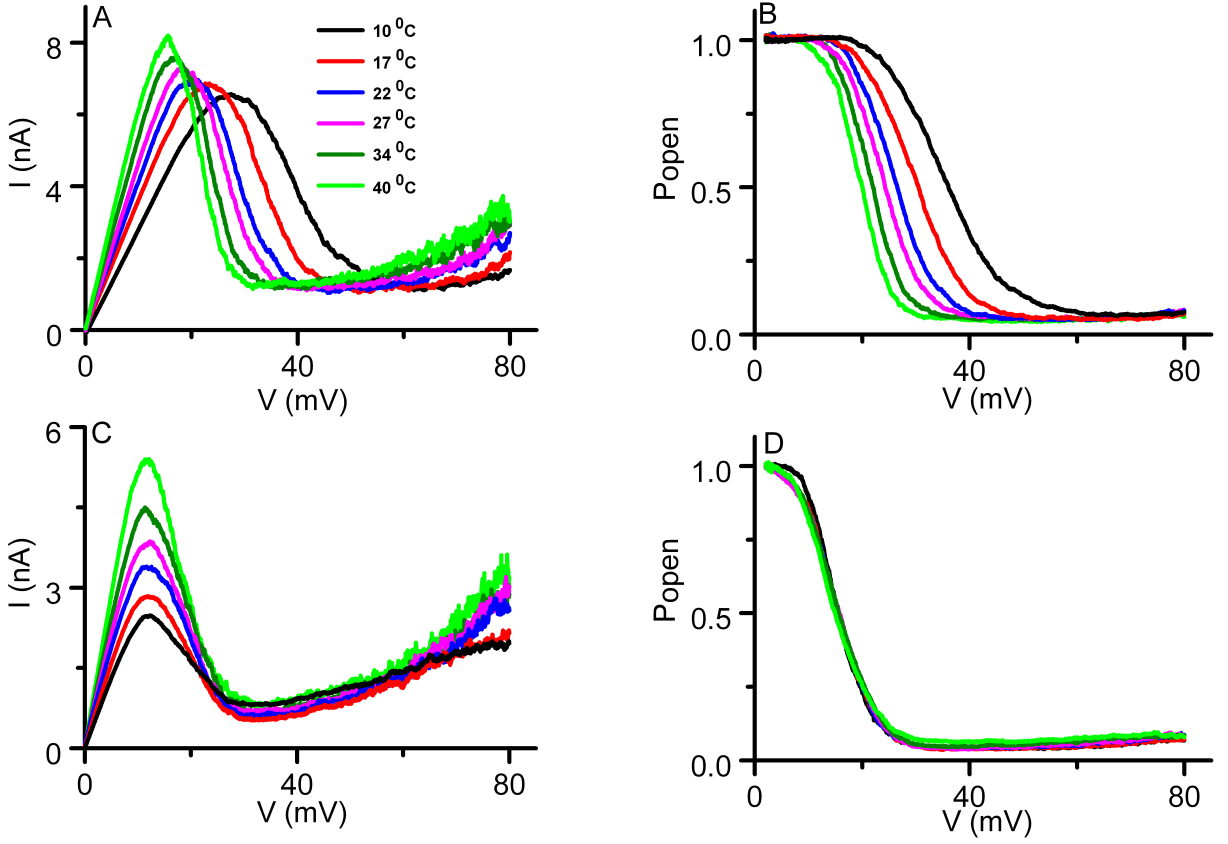
A
10 °C
17 °C
22 °C
27 °C
34 °C
40 °C
I (nA)
V (mV)
B
Popen
V (mV)
C
I (nA)
V (mV)
D
Popen
V (mV)